Eur. Phys. J. D **13**, 93–107 (2001)

THE EUROPEAN PHYSICAL JOURNAL D

EDP Sciences

On the observation of decoherence with a movable mirror

R. Folman[1,a], J. Schmiedmayer[1], H. Ritsch[2], and D. Vitali[3]

[1] Institut für Experimental Physik, Universität Innsbruck, Technikerstraße 25, 6020 Innsbruck, Austria
[2] Institut für Theoretische Physik, Universität Innsbruck, Technikerstraße 25, 6020 Innsbruck, Austria
[3] Dip. di Matematica e Fisica, and Unità INFM, Università di Camerino, 62032 Camerino, Italy

Received 2 December 1999 and Received in final form 6 April 2000

Abstract. Following almost a century of debate on possible "independent of measurement" elements of reality, or "induced" elements of reality – originally invoked as an *ad-hoc* collapse postulate, we propose a novel line of interference experiments which may be able to examine the regime of induced elements of reality. At the basis of the proposed experiment, lies the hypothesis that models of "induced" elements of reality should exhibit symmetry breaking within quantum evolution. The described *symmetry experiment* is thus aimed at being able to detect and resolve spatial symmetry breaking signatures. The proposed experiment stands at the edge of present day technological abilities and will be, so we believe, realizable in the near future.

PACS. 03.65.Bz Foundations, theory of measurement, miscellaneous theories (including Aharonov-Bohm effect, Bell inequalities, Berry's phase) – 42.50.Vk Mechanical effects of light on atoms, molecules, electrons, and ions – 42.50.Dv Nonclassical field states; squeezed, antibunched, and sub-Poissonian states; operational definitions of the phase of the field; phase measurements

1 Introduction

The loss of the ability to consistently use the word particle (referring to a classical point of mass), is of course one of the well-known implications of quantum mechanics, and stands at the base of what has been named the "measurement problem". Instead, we make use of a mathematical entity called the wave function, which is allowed superpositions, which cannot describe our classical notion of reality. This is perhaps most readily exhibited in the double slit experiment. Indeed it was Feynman who described the double slit experiment as "... it contains the only mystery" [1]. It is also a matter of general knowledge that many of the important contributors to the theory were not satisfied with this state of affairs. They felt that some level of independent reality does in fact exist, and connects to quantum expectations through some set of local or nonlocal hidden variables. Just to mention a few, de Broglie for example, tried to formulate alternatives such as the "guiding wave" or the "double solution" models, which were, by his own admittance, unsuccessful. Nevertheless, until his last days, he continued to believe that a theory maintaining some sort of particle independent reality should be found [2]. Bohm, went a step further by publishing a consistent formalism which enables the existence of a particle, while reproducing standard quantum expectations [3]. Indeed some, such as Bell, have taken the view that Bohm's success presents a superior interpretation, while others thought differently [4]. Einstein with the EPR paradox, Schrödinger with the cat enigma, and other important contributors, were also uncomfortable. We refer the interested reader to some of the many available textbooks on the interpretation of the past and possibilities of the future regarding quantum theory [5].

Simply stated, the measurement problem may be described as follows: if there are two possible pointer positions (in the measuring apparatus), the superposition principle maintains that any superposition of those two pointer positions must also be a possible state. However, such superposition states of macroscopic pointers have never been observed [6]. In the language of the above single particle double slit experiment: the superposition principle does not allow us to use the word particle if we are to describe the evolution of the quantum system. However, the outcome of the experiment necessitates the use of the word particle in contradiction to the superposition principle. Even if one accepts Bohr's escape route, which divided the world into quantum and classical, one is left with a fuzzy, impossible to define, border between the two.

A second class of models attempting to resolve the measurement problem invokes "induced classical reality" rather than "independent reality". Here it is important to clearly define what one means by the words "induced" and "classical reality". By "induced" we simply mean the emergence of "classical reality" as an outcome of processes, which depend on parameters such as time and mass (or number of particles). By "classical reality" we mean the emergence of statistical mixtures instead of

[a] e-mail: ron.folman@uibk.ac.at

superpositions. Namely, the Ball was "here *and* there" and now it is "here *or* there". The exact location (here/there) of the Ball has randomly been chosen by nature but it has been chosen. It makes no difference if this location has been uniquely chosen in one world or in one out of many. In the world in which we make the experiment, the location has been chosen independently of any observer or measuring apparatus. The latter must be at the basis of any model attempting to explain why we see a classical world.

Furthermore, it makes no difference if one wants to stay within the framework of quantum theory and unitary evolutions and thus can only speak of the emergence of statistical mixtures rather than one unique location. A statistical mixture is only a measure of our ignorance, and any model wishing to describe the emergence of the classical world independent of man and his machines, must agree that one location has been *realized*. We will later see that indeed, whether one uses the language of a localized wave function or of a statistical mixture, makes no difference to the experimental prediction of our proposed experiment.

One example of such a model would be the spontaneous localization through the GRW (Ghirardi, Rimini and Weber) mechanism and its successors [7]. Another example is what Folman and Vager described as the "non-passive Bohmian particle" [8], which Bohm described as a particle having influence on the wave function "... so that there will be a two way relationship between wave and particle" [9]. In this scenario, the wave function, which determines the evolution of the system, is gradually distorted by the particle and its location – away from the form of superposition. There are numerous other hypothesized models such as gravity based induced decoherence (see Penrose [10]), but perhaps the most well-known model of this class of "induced reality" models, is that of a "collapse" due to the coupling to the environment. This is usually referred to as *Decoherence*, which states in essence that the reduced density matrix von Neumann called for (having no off diagonal elements) may be arrived at naturally through the entanglement of the system and the detector to the environment (see Zurek [11]). Thus, in addition to the usual parameters of time, mass and spatial separation (which are needed if we are to explain our observations), *Decoherence* correlates the loss of coherence to the coupling onto the environment.

The question we would like to address in this note, is how may we try and experimentally investigate the second class of models so that their general validity would be asserted, and also, how may we possibly differentiate between them. Furthermore, we would like to explore these questions in the x-space (which is by admition of these models the important space [12]) and with macroscopic objects so as to be able to really examine the border Bohr was trying to define. The latter requires of course the ability to observe the macroscopic system before and after it decoheres.

To conclude, the motivation for such an experiment is three-fold.

a. To observe the evolution of an isolated macroscopic quantum system (an interesting observation in its own right).
b. To observe the transition into a classical system through the process of Decoherence.
c. If the coupling to the environment does not mask [13] in magnitude and time other possible mechanisms such as GRW, to try and experimentally observe other mechanisms as well.

2 The experimental problem

There are two major experimental problems concerning the observation of localization as a function of time, mass and the variation of the coupling to the environment.

Problem I. *It is hard to observe a quantum system without coupling to it and initiating uncontrollable decoherence as part of the measuring process [14]. Namely, it is well-known that measuring whether the Ball is "here* or *there" results in the Ball being "here* or *there". Hence, if we are to learn about the inherent decoherence mechanisms of nature such as the coupling of the environment to our system, we are faced with the contradiction in which we are not allowed to measure that which we are trying to observe (namely decoherence in x space) i.e. the coupling between our x eigenstate apparatus will mask the weaker localization processes, which we want to investigate.*

Resolution I. *Use non-demolishing measurements in which the system's unitary evolution in the base of your choice (in our case it will always be x), is not affected by the measurement.*

Here, it is interesting to note, that following a suggestion for a gravitationally induced collapse model [10], Schmiedmayer, Zeilinger and colleagues have also investigated the idea of monitoring the behavior of a coherent system in order to observe decoherence [15]. They made the point that any "welcher weg" information would have to be erased or not invoked in the first place, for such an experiment to be performed. As will be shown in the following, this is exactly the idea behind our proposed experiment and why we consider it to be non-demolishing (see Working assumption II).

Problem II. *So far experimentally, observed coherent systems in a state of spatial superposition are particles, atoms or molecules. These are either too light to observe localization in the time frame of the experiment, or, their mass is fixed, making it hard to determine the proportionality of localization to mass. Furthermore, particles in well defined states of spatial superposition, are usually in motion, which makes the control of their environment a hard task.*

Resolution II. *Keep particles only as probe while turning the set-up into the observed system, which is in a well defined spatial superposition, with a variable mass and environment.*

Finally we note that the affect of the environment, as well as other parameters, on localization has long been the subject of experimental interest, but as far as we know, with no conclusive results regarding x-space and massive

objects. For example, one such on going experimental effort concerns the handedness of chiral molecules [16]. Another experiment investigated decoherence of an "atom-cavity field" entangled state, where the macroscopic element was that of the phase difference between the cavity fields [17]. Recently, several schemes have been suggested aiming at directly investigating massive objects [18]. In this context, micro movable mirrors (which are also discussed in this paper) have also been discussed extensively [19] and realized [20]. This, however, as far as we know, only in the context of cavity walls. In the following we present what is to the best of our knowledge a novel type of experimental procedure in the context of localization, which may shed new light on the processes initiating it. It relates to the issue of symmetry in quantum phenomena, which is an underlying feature of the theory. Namely that the difference between classical and quantum states is that the phase between possible positions is lost, and hence symmetry in space may exist between probabilities but not amplitudes. In other words, in the transition from Quantum to Classical, symmetry is conserved only as a statistical average in the form of a statistical mixture (see Working assumption I in the following).

3 The experimental assumptions

In reference [8], Folman and Vager proposed to incorporate the two experimental resolutions described above by utilizing a *symmetry experiment* with a movable mirror, to observe localization and decoherence. Their point was that localization could be observed, not only by the breaking of energy conservation of our isolated system (producing photon emission) – as suggested by Pearle and Squires [7], but also by the breaking of symmetry. However, they gave little consideration to the experimental feasibility. In this note, we expand the idea of the *symmetry experiment* to include all models of the second type. We also include different versions of the experiment, which may be more realizable and conclusive. Finally, we also present initial calculations to examine the experimental feasibility.

Before describing the experiment, we lay down the foundation by emphasizing several fundamental assumptions.

Working assumption I. *The invoking of localization, via models of the second type, destroys amplitude (wave function) symmetry, even when we have not gained any knowledge of which of the possible x-states has been occupied. Namely, symmetric or anti-symmetric states become asymmetric. Consequently, eigen-states of parity are lost.*

This is obvious in the case of a collapse of a symmetric superposition into one of the two locations (as proposed by the GRW mechanism). In such a case, the resulting wave function is asymmetric. However, even in the case of *Decoherence* where only a statistical mixture of the two positions emerges, one observes symmetry breaking *e.g.* applying the parity operator on a two-by-two symmetric density matrix (all elements equal 1/2) and taking the trace, gives an average of +1, while repeating the same procedure for a symmetric mixture (off diagonal elements are 0 and diagonal elements are 1/2) gives a measurement average of 0. For example, it is well-known that for localized chiral molecules having well defined handedness, parity is not a good quantum number. In general, if this working assumption were not valid, then it would follow that a classical reality or at the very least the change of the wave function, independent of man and his apparatuses, has not been invoked by this second class of models, although this was their main goal [21]. Indeed, symmetry of the wave function must be lost as the loss of the relative phase is an essential part of all localization schemes.

Working assumption II. *Measuring parity does not localize (i.e. decohere) the system in x-space.*

This working assumption is self evident as the spatial spread of the wave function remains unchanged by the parity operator. Using once again the example of chiral molecules, measuring parity does not induce handedness. In another example, one is able to see x-space interference fringes in the double slit experiment, although one knows the parity of the incoming beam. Similarly, Scully *et al.* [22] have shown in a "quantum eraser" experiment, that sending excited atoms through optical cavities which serve as "welcher weg" detectors, does not destroy coherency if the only knowledge gained is the parity (*i.e.* both cavities were exposed to the same photon detector), and no knowledge is available regarding at which cavity the photon has been released.

Working assumption III. *There are no other possible causes for symmetry breaking in our finite system, aside from the hypothesized localization. Namely, if the set-up is symmetric and the Hamiltonian conserves parity (we neglect the weak force), any sign of symmetry breaking must be due to localization.*

Again, if this was not so, we would have observed symmetry breaking long ago, due to a breaking term in the evolution operator. Remark: there could of course in principle be interactions between our finite system and its surroundings, that would change the symmetry of the former with no connection to localization (decoherence). However, as will be shown later on, our experiment is sensitive to the source of the symmetry change. Hence, we are able to exclude in this working assumption, symmetry breaking signals which are simply due to symmetry exchanges with the out-side of our system. Namely, we are able to exclude from our signal processes such as heating (*i.e.* the formation of a thermal state) or coherent excitation (*i.e.* the formation of a superposition of bound states), and conclude that what ever symmetry breaking signal remains, must be due to localization (*i.e.* the formation of a mixture in position from the coherent ground state).

Following working assumptions I, II and III, we set out to search for symmetry breaking effects.

4 The experiment

The first stage of the experiment includes the preparation of a symmetric initial particle wave function Φ_i. This may be done by the apparatus presented in Figure 1. D1 and D2 are two particle detectors (if needed, with the ability

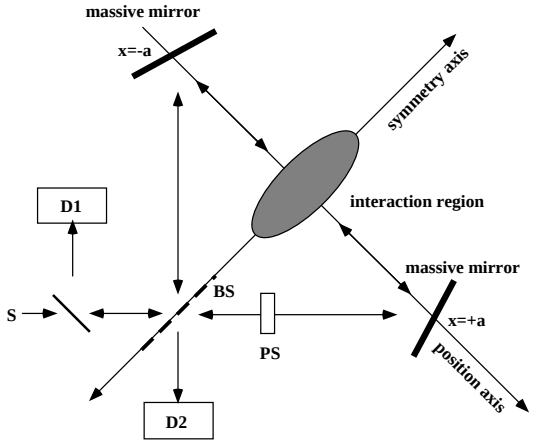

Fig. 1. The closed loop interferometer. As the interaction region C is transparent, both paths are identical as they are one of the same. S, D1, D2, BS, PS are the particle source, the two detectors, the beam splitter and the phase shifter, respectively. The eigen-states of the measuring system are parity eigen-states. While transversing the apparatus, the initial symmetric wave function is exposed to the influence of the relevant parameters such as time, spatial separation, and environment, or any other symmetric interaction which we place at the interaction region C. There is no reason for the outgoing wave function to lose its initial symmetry and hence we expect no "click" in detector D2, unless loss of coherence due to localization has occurred.

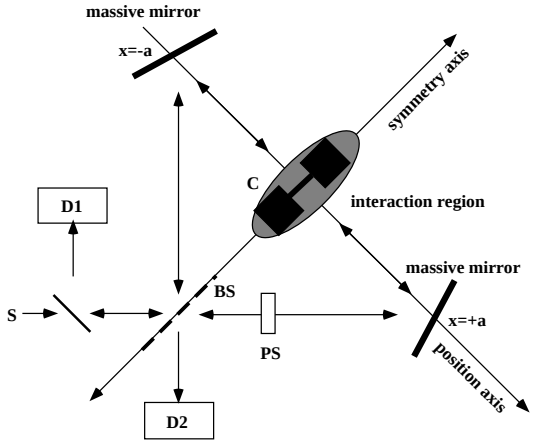

Fig. 2. The open loop interferometer. Here, in addition to what has been described in Figure 1, we position a two sided foil mirror, held in an harmonic potential, into the interaction region C. Hence, we entangle the transversing particle to the state of the set-up, which is also in a well-defined quantum state with a well-defined spatial uncertainty. Thus, we are able to examine the quantum evolution of a macroscopic system. Using parity eigen-states to measure the state of the outgoing particle, we learn about the decoherence of the set-up, without affecting it.

to measure the particle's energy). S is the particle source. The phase shifter (PS) cancels the phase difference introduced by the beam splitter (BS), between the phase of the transmitted wave and that of the reflected. We of course assume a perfect 50%/50% BS and a PS which is invariant to changes (as is the BS) in the wave number. The preparation apparatus then also serves as the measurement apparatus with parity eigen-states.

The interaction region may hold several types of experiments.

4.1 The closed loop interferometer

This interferometer has the distinct advantage of ensuring symmetry, as its two optical paths are one and hence identical.

In the simplest case, where we set out to examine induced collapse independent of the environment, the interaction region may stay empty.

The two important parameters are time and mass (or number of elementary particles). Mass could be controlled by the size of the particles we send into the interferometer, and time by their velocity and the size of the interferometer.

Dependence of localization on the environment, may be examined by introducing a symmetric interaction which would keep the Hamiltonian invariant to space inversion along the position axis (*e.g.* magnetic or electric field or modulating crystal).

In all these cases, a "click" in D2 would mean that the single particle initially arriving from S with a symmetric $\Phi_{\rm i}$ has now transformed to a final $\Phi_{\rm f}$ which is anti-symmetric or asymmetric. As there are no reasons for $\Phi_{\rm f}$ to be anti-symmetric (see assumption III) we conclude that $\Phi_{\rm f}$ is asymmetric. In the single particle case some of the asymmetric photons would end up in detector D2, telling us that the particle was localized. This could be verified by repeating the experiment with a multi-photon pulse and observing hits on both detectors. As the collapse postulate cannot be responsible for the observed symmetry breaking (see assumption II), we conclude that we have observed induced localization (see assumption I).

4.2 The open loop interferometer

If we are not able to achieve coherent symmetric states with very massive particles (needed if we are to observe induced localization on the time scale in which the particles transverse the apparatus), or if we are unable to satisfactorily control the particles' environment while they are in motion, we would have to resort to a more complex experimental scheme which we describe here as the open loop interferometer. Different from the previous interferometer, here, the interaction region is blocked by a second symmetric quantum system. In this scheme, we loose the simplicity of having only massive reflections but we gain the possibility of observing a quantum object in a localized potential, for long periods of time and with the ability to control its mass and environment. Consider, for example, the set-up of Figure 2.

Here, a mirror has been placed in the interaction region. In this example, the mirror in the interaction region (C) is actually a two sided reflecting foil which is in an harmonic oscillator potential. Neglecting inner degrees of freedom, such as those corresponding to the Debye-Waller factors (since it is known that these factors also exist in massive mirrors but still they reflect coherently), we take account only of the center-of-mass of the foil, and note that it is in a parity eigen-state (say, the even ground state $\Psi_{\rm i}$). We further note that $\Psi_{\rm i}$ is symmetric with respect to the same symmetry axis as $\Phi_{\rm i}$. Namely, they are both symmetric with respect to the axis that lies in the plane of the beam splitter, which is also the plane of the average position of the foil.

As the total initial wave function $\Omega_{\rm i} = \Phi_{\rm i} \otimes \Psi_{\rm i}$ is symmetric and as the Hamiltonian is parity conserving and invariant under the combined two reflections of the x', x'' coordinates of the two wave functions, the final total wave function $\Omega_{\rm f}$ must also be symmetric and hence it may be defined as

$$\Omega_{\rm f} = \sum \Phi_{\rm s} \otimes \Psi_{\rm s} + \Phi_{\rm as} \otimes \Psi_{\rm as} \qquad (1)$$

where "s" and "as" stand for symmetric and anti-symmetric, and the summation is over all possible foil states (the latter is a general consequence of parity conservation. For a formal derivation with the specific coherent reflection Hamiltonian, see Appendices). We note that these arguments are independent of the mass of the foil C. It should also be explicitly stated that we have been discussing parity although what is clearly evoked are reflection symmetries. As the relevant parameters of position and momentum all point along the position axis (see figures), the problem is one dimensional and a rotation which differentiates reflection symmetry from parity has no effect. Consequently, the two symmetries may be considered one of the same. The polarization of light may also be made to point along the position axis, or alternatively, the set-up could be made invariant to the polarization.

Let us conclude. Changing the observation time, or the environment or the mass of the foil, would allow us to investigate the process of induced localization. Registering a "click" in detector D2 and at the same time knowing that the symmetry change the foil has undergone does not maintain the final symmetry requirement of equation (1), will indicate the occurrence of symmetry breaking and of induced localization. Again, using a multi-photon pulse may enable a complementary check to the single photon probe.

Finally, changing the set-up slightly, one may prohibit localization signals from detector D2 (*i.e.* only anti-symmetric excitation events would "click" at D2), and hence establish yet another complementary check on the source of the deviations. This is what was referred to in the remark of Working assumption III, when it was stated that we are able to differentiate between symmetry breaking coming from the formation of a position mixture in the ground state, and between other symmetry changing sources such as heating or coherent excitation by the surroundings of the system. As an example of such an apparatus, we present the set-up of Figure 3. Here, massive mirrors A and B maintain the loop actually closed.

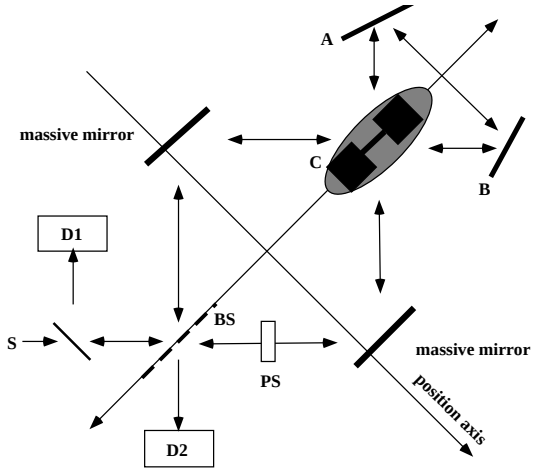

Fig. 3. The semi-closed loop interferometer. Here, we add two massive mirrors to the set-up of Figure 2, so as to close the interferometer loop. Consequently, an off center localization of the foil mirror, would not hinder the equality of the two optical paths. This, makes the set-up insensitive to localization signals while still sensitive to external symmetry changing excitations of the mirror foil, whether thermal or coherent, due to bad isolation of our system, or apparent symmetry breaking which is simply due to the initial state of the mirror not being in the ground state (*e.g.* insufficient cooling). Hence, this set-up will enable further verification of our understanding of the results.

We end this section by noting that the above presented experimental procedure should be able to investigate any model in which decoherence is also a function of mass, time and/or state size. As these parameters are essential in all models of the second type, we conclude that the *symmetry experiment* may be utilized to investigate the full range of models of this class.

5 Some numbers

Let us make some initial calculations for the open loop interferometer, to show what kind of experimental procedure would be needed to realize this experiment.

For the purpose of illustration, we start with the extreme and simplistic demands that (a) we are in the high resolution regime where the photon wave length is much smaller than most possible mirror position deviations due to localization, and (b) the foil is not excited during the interaction with the photon *i.e.* its symmetry is not changed by the foil-photon interaction. Let us elaborate:

(a) We demand that the wavelength λ of the probing particle be much smaller than the mirror localization position $X_{\rm loc}$ which is of the order of the width W of the ground state at interaction region C. If this were not so, the localization relative signal would behave as $I_2/I_1 = \tan^2(4\pi W/\lambda)$ where I_1 and I_2 are the photon intensities at detectors D1 and D2, coming from a localization event. Consequently, the absolute signal (D2)

would become smaller and smaller. A derivation is given in Appendix A. For now, let us then assume an harmonic potential so that $W = \sqrt{\hbar(n+1/2)/(m\omega/2)} \gg \lambda$ (which only differs by a factor $\sqrt{2}$ from the frequently used $W = \sqrt{\langle x^2 \rangle}$). If we take for example the photon as a probing particle, and assume that we are able to use light from X-ray to red at a wavelength of 0.1−1000 nm, and system C is say in the ground $n = 0$ state, we find that for X-ray (red):

$$\sqrt{\frac{\hbar}{m\omega}} \gg 0.1 \text{ nm } (1000 \text{ nm}) \text{ or } m\omega \ll 10^{-14} \ (10^{-22}). \tag{2}$$

(b) We demand that excitations be suppressed by the maximally allowed energy transfer. We note that the maximum energy transfer by the photon cannot exceed that allowed by momentum conservation, namely: $2(\hbar k)^2/m \approx 8\times10^{-47}/m$ which would mean in the case of a 10^8 nucleon oscillator, an approximate transfer of 8×10^5 Hz. This should be compared with the 10^4 Hz maximally allowed energy spacing, under condition (2). This ratio between the maximum transferred energy by momentum conservation and the maximally allowed harmonic energy spacing is constant for all masses and wavelengths, and has the value of $(2(\hbar k)^2/m)/(\hbar^2/m\lambda^2) = 8\pi^2$. Namely, momentum conservation does not prohibit the harmonic oscillator system from being excited to at least one level above. As we have taken $|k_\mathrm{i}|$ and $|k_\mathrm{f}|$ to be identical, the latter calculation is of course only valid in the limit of massive objects which due to their mass do not receive significant recoil energy. For exact numbers, we would need to make the quantum calculation which is simple enough. For example, taking the ground state as the initial state, the probability for the foil not to be excited is simply the well-known Debye-Waller factor $P_{0\to0}$ which is for the case of the X-ray, and again under condition (2), smaller than

$$\exp(-\hbar^2(2k)^2/2m\hbar\omega) = \exp(-8\hbar\pi^2/\lambda^2\ 10^{-14}) \approx 10^{-35} \tag{3}$$

(the full calculation may be found in Appendix B). We see that the energy transfer can actually be equal to many times the harmonic energy spacing. Hence, we come to the conclusion that working within the "high resolution" $W \gg \lambda$ regime and with non-excitation events, is not feasible (this is true for both X-ray and red light).

We therefore move on to more realistic scenarios and discard our two initial demands. It is clear that in order to perform the experiment, it is not enough to measure the symmetry of the outgoing photon; one must also know the symmetry change of the mirror. For a single particle experiment, we are left with two main options:

(a) calculate the expected foil excitation rate (to levels of different symmetry) due to the foil-photon interaction and subtract that rate from the signal at D2;
(b) know whether the mirror has been excited and if so to what level, by measuring also the energy of the outgoing photon at D2.

Let as elaborate: (a) here, we intend to gain control over unwanted foil excitations by simply preparing an experimental procedure in which $P_{0\to n(\mathrm{odd})}$ (*i.e.* the expected excitation signal at D2) is well-known. Namely, by knowing what the expected "noise" in D2 is (*i.e.* the anti-symmetric photons coming from excitation events), one can differentiate between the signal at D2 and the "noise". However, for the experiment to be feasible, one must make sure that the noise does not overwhelm the signal – especially now that the strength of the signal is not ensured, as we no longer enforce condition (2). Hence, we need to calculate the values of the ratio

$$R = \frac{1 - P_{0\to n=0,2,4,\ldots}}{g(\tau)I_2/(I_2+I_1)} \tag{4}$$

where,

$$\frac{I_2}{I_2+I_1} = \int_{-\infty}^{+\infty} f(X_\mathrm{loc}) \sin^2(4\pi \frac{X_\mathrm{loc}}{\lambda}) \mathrm{d}X_\mathrm{loc} \tag{5}$$

is the average probability of receiving a click at D2 when a localization has occurred, where $\sin^2(4\pi X_\mathrm{loc}/\lambda)$ was calculated in Appendix A, and where the average is over,

$$f(X_\mathrm{loc}) = \Psi_0^\dagger(X_\mathrm{loc})\Psi_0(X_\mathrm{loc}) \tag{6}$$

which is identical to the initial state position probability distribution, which is simply for our example, the harmonic ground state Ψ_0.

$g(\tau)$ is the localization probability after time τ, which will be different for different localization models. Keeping to a general frame, we will in the following set $g(\tau) = 1$ which simply means that between preparation and measurement one waits long enough. Obviously, to differentiate between different localization models one would then shorten τ or change the foil mass and temperature in order to find which model fits best with the observed $g(\tau)$.

Finally, we note the obvious which is that once R is calculated, one may easily extract the expected deviations in D2 from the signal expected from the standard symmetry breaking source referred to above as "noise". Once again, these deviations are what our experiment is searching for.

(b) Here, we intend to identify which clicks at D2 are simple excitation "noise" by measuring also the energy of the detected photon at D2. If the energy difference between the initial and final photon corresponds to a foil excitation between levels of different symmetry (*e.g.* from the ground state to the first odd state), this event will be discarded as having a standard quantum origin. Indeed, this is a straight forward option which does not have any dependence on the validity of calculations as those suggested above. Furthermore, as in this option the symmetry change of the mirror is directly measured, it will not be sensitive to external sources of symmetry breaking, such as those discussed in work assumption III, and will thus not need further verification set-ups like that presented in Figure 3. The latter and the fact that the mirror does not have to be cooled to its ground state (for the same reason), are the clear advantages of this option. However, as will be

shown, limited available detector energy resolution, limits its usefulness.

In the following section we investigate these two propositions, and also touch upon the issue of a multi-particle probe.

6 The proposed experimental procedure

In this section we elaborate further on the ways in which the experiment may be performed. As an example we take the probe particle to be a photon. These are two options which will be dealt with in the section.

a. Single photon experiment, where the search will be for deviations in the overall detector intensities i_{D1} and i_{D2} from the standard quantum ratio between symmetric and anti-symmetric photon final states due to expected photonic foil excitations. Here, many repetitions of the same single photon experiment will enable us to directly measure the ratio between symmetric and anti-symmetric final states, which in turn is a consequence of the excitation probabilities. Hence, we will be able to measure the excitation probabilities in a quantum macroscopic system and to be sensitive to deviations which are due to localization. Remark: even if for some reason (*e.g.* coherent excitation of the foil to higher odd states by the environment) our calculation of $P_{0\to\mathrm{odd}}$ is an under estimate (as it was estimated for the isolated system), one would still be able to detect deviations due to localizations, as explained in the remark of Working assumption III and the text concerning the set-up of Figure 3.

Starting from the ground state one may also consider a multi-photon (pulse) experiment, where $i_{\mathrm{D1}}/i_{\mathrm{D2}}$ are different for a symmetric outgoing pulse, an anti-symmetric outgoing pulse and an a-symmetric outgoing pulse. Here, a localization event may be detected by the abnormal intensity of a single pulse split at the beam splitter. The immediate and clear advantage of a multi-photon pulse experiment, is of course the fact that a single experiment (*i.e.* one pulse) can detect a localization. The clear signal would be an intensity split ratio which is classically related to the X_{loc} of the localization, as described in Appendix A. Again, integrating over all observed localization signals, should of course be in agreement with the density function of the ground state. The important issue at hand is: what would be the signal coming from non-localization events (coherent excitation and non-excitation events). We leave further discussion of this option to a dedicated note.

b. Single photon energy measurement experiment, where the outgoing photon discloses both its symmetry, and that of the foil. See elaboration in the following.

Experiment a: to see if this experimental procedure allows for a reasonable signal over noise ratio, and for what values of the parameters it does so, we calculate R as a function of m, λ and ω. As mentioned before, we ignore the internal degrees of freedom (based on the coherent reflection of visible light mirrors and X-ray gratings) and treat the center-of-mass motion of the mirror. Namely, as in the Mössbauer effect, there are no excitations of internal degrees of freedom. Whether or not this is a good approximation, depends on the specifics of the incoming wave and the mirror, including its thickness and material (see in the following, discussion regarding the extinction coefficient in section "Mirror, vacuum and preparation"). With the above assumption, and in the Lamb-Dicke limit (see full calculation in Appendix C), we find R to be

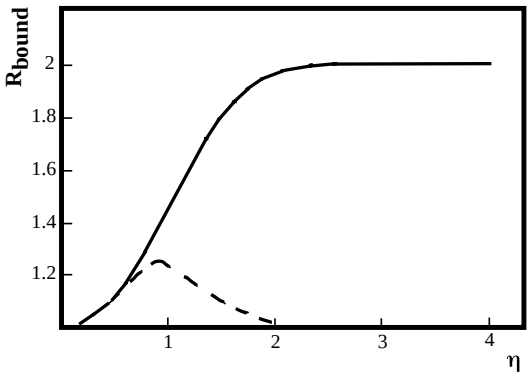

Fig. 4. R_{bound} as a function of η, which in turn is a function of the foil mass and frequency, and the wavelength of the light, with the relation $\eta = 4\pi W/\sqrt{2}\lambda = (4\pi/\lambda)\sqrt{\hbar/2m\omega}$. The dashed line qualitatively presents the general expected form of R (see text). Note that the Lamb-Dicke limit is only valid for $\eta \ll 1$. One should also note that the signal itself $I_2/(I_2+I_1)$ falls as η approaches zero, but it maintains reasonable values $(0.01-0.43)$ for η between 0.1 and 1 (see Appendix C.2).

$$R = \frac{\eta^2 + (\text{higher orders})}{I_2/(I_2+I_1)} \tag{7}$$

where η is the Lamb-Dicke parameter $\sqrt{E_{\mathrm{r}}/\hbar\omega} = 4\pi W/\sqrt{2}\lambda$ (E_{r} is the recoil energy), where we have neglected factors which appear in Appendix C.1, and where the denominator is calculated in C.2.

We note that the Lamb-Dicke regime may be an advantageous one as the mirror frequencies are higher and perhaps easier to achieve, but mostly as the energy level spacing is larger and hence cooling to the ground state is a less formidable task. Of course, whether or not a system is in the Lamb-Dicke limit depends on the chosen experimental parameters. Out side the Lamb-Dicke regime, one may easily evaluate the qualitative behavior of R by first looking at the upper bound of R, namely,

$$R_{\mathrm{bound}} = \frac{1 - P_{0\to 0}}{I_2/(I_2+I_1)} \tag{8}$$

(this simple enough calculation is also presented in Appendix C). The rather striking "inversion" in R_{bound} seen in the Figure 4, is dependent on the mass of the foil, its frequency and the frequency of the impinging light, only *via* the parameter η! For X-ray and 10^{15} particles, the frequency of the foil as a function of η is approximately $f = 10^{-1}/\eta^2$ Hz. This means that in order to observe the inversion in R_{bound}, one would have to work in the regime of low (but realizable) frequencies. However, it is expected that the "inversion", would not be experimentally observable in full; as can be readily

seen from the Debye-Waller expression in equation (3), which simply equals $\exp(-\eta^2)$: $P_{0\to 0} < 10\%$ ($> 90\%$) for $\eta > 1.5$ (< 0.3). One may then roughly assume that for the first case $1 - P_{0\to 0} \to 2\ (1 - P_{0\to n=0,2,4,...})$ since $P_{0\to 0} \to 0$ and $P_{0\to 0,2,4,...} \to 1/2$. Similarly for the second case, $1 - P_{0\to 0} \to 1 - P_{0\to n=0,2,4,...}$ since $P_{0\to 0} \to 1$ and $P_{0\to 0,2,4,...} \to 1$. Hence, we find respectively that for $\eta > 1.5$: $R \to \frac{1}{2} R_{\rm bound}$, and for $\eta < 0.3$: $R \to R_{\rm bound}$. Consequently, this means that instead of observing the full "inversion" one should be able to observe a peak in the value of R for η in the region of 0.9. This is qualitatively described in Figure 4 as well.

As $R \leq R_{\rm bound}$, the experimental sensitivity for the various values of the experimental parameters, will be better than that indicated by the bound. Observing the above form of the dependence of R as a function of η, may serve as yet another verification that the deviations that are observed at detector D2, indeed originate from localizations. For example, for a constant 10 Hz foil frequency, the range of $0.1 < \eta < 2$ could be scanned by simply changing the mass of the foil in the range $10^{12} <$ no. of particles $< 10^{15}$.

As for red light, one can easily see that for 10^{15} particles $f = 10^{-9}/\eta^2$ Hz, which means that although one may perform the experiment with red light (reasonable anti-symmetric "noise" to signal ratio), one is not able to explore the "inversion" regime, as the needed foil frequency would be far below 1 Hz (which would probably be mechanically hard to achieve. See following section: "Mirror, vacuum and preparation"), or alternatively, the needed foil mass would be extremely small, and in order to observe decoherence, one would have to maintain a stable and isolated experiment, for long periods of time. Nevertheless, if one has enough statistics, one may try and observe the logarithmic behavior of R for smaller values of the η parameter. In any case, it should be once again noted, that as the observation of the peak or logarithmic behavior are mere verifications, the experiment itself could be performed with a large range of light and mirror frequencies.

Finally, we add that although in general, localization times in the different models depend on the number of particles or the mass, some models also take into account the spatial separation. For our bound mirror foil, the larger the mass, the smaller the ground state size and hence the position uncertainty, which constitutes the separation between the different possible positions. Thus increasing the mass will on the one hand shorten the decoherence time but on the other hand prolong it. It is therefore clear that the exact parameters needed in order to achieve decoherence on the experimental time scale, are model dependent. However, it is also clear that any model attempting to explain the "localization of the pointer" must also predict the localization of our mirror. It remains to adjust the experimental parameters so that the predicted decoherence times are within the experimental time scales.

Experiment b: as explained in the previous section, one clear advantage of this option is the fact that the symmetry change of the mirror is directly measured, by measuring the energy loss the photon clicking at D2 has suffered, and assuming that the only possible transfer of energy is for the excitation of the mirror foil. This avoids the need for further verifications, such as that suggested in Figure 3, excluding other sources of symmetry breaking (such as some external mechanism through which the mirror is excited) which are referred to in work assumption III. Another clear advantage is the bypassing of the need for cooling the mirror into an initial ground state; As the symmetry change of the mirror is now measured directly, the initial symmetry of the mirror is not crucial any longer. Let us elaborate. As the energy level spacing of the mirror $\Delta E = \hbar\omega$ is known, being able to resolve the energy loss of the photon with an accuracy much better than ΔE, would enable us to know how many energy levels the mirror has jumped. Obviously, an odd number jump would mean a symmetry change in the mirror while an even number jump would mean that the out going photon must maintain its initial symmetric form, unless of course a localization event has occurred.

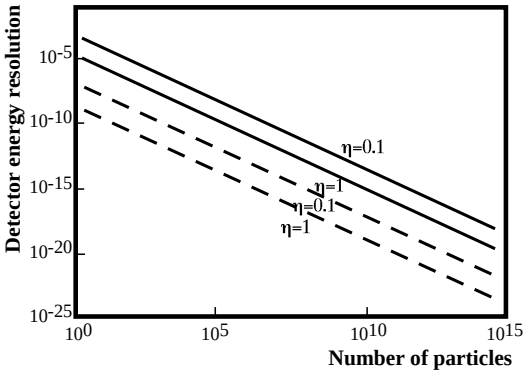

Fig. 5. Needed energy resolution $\Delta E/E_\gamma$ as a function of the number of foil nucleons, for the two examined extremes of the feasibly used light spectrum: X-ray and red (in dashed line). As an example, two η values, which correspond to reasonable suppression factors of the localization signal (see caption of Fig. 4), are given.

Taking as the observation limit a detector energy resolution of $\Delta E = \hbar\omega$, the needed relative energy resolution $\Delta E/E_\gamma$ in order to be able to take account of the foil excitation (*e.g.* make use only of non excitation events), as a function of the number of particles in the foil, is presented in Figure 5.

As can be understood from the figure, for a constant η the needed resolution is harder to achieve as the number of particles grows. This is a direct outcome of the definition of η in which for a constant η, the number of particles is inversely proportional to the oscillator frequency. Obviously, as the mirror oscillation frequency becomes smaller, it will be harder to resolve from the photon energy measurement, what excitation has occurred in the foil, as the energy level spacing becomes smaller. Nevertheless, in the following it is shown that present resolutions already enable us to perform some versions of the experiment.

We now turn to discuss some technical but nevertheless crucial aspects of the experiment.

7 Mirror, vacuum and preparation

In the previous paragraphs, we calculated the excitation probability without taking into account the specific features of the mirror. Obviously, a full account of the mirror features has to be made. This is not just a matter of the mirror's material. The mirror's thickness may also dominate the ability of the mirror to reflect or to have a wanted ground frequency (*e.g.* of the order of the example 10 Hz). In the following we present some preliminary classical considerations which will have to be followed when constructing the mirror.

For example, if one takes an atom to have a volume of 10 cubic Angstrom, then a 1 mm^2 mirror, would have a thickness of only 10−1000 atom layers for 10^{13} to 10^{15} atoms. The question then arises if such a small thickness can have non-negligible reflectance. Taking perpendicular impinging beams (*i.e.* parallel and perpendicular polarisations give rise to the same border reflection), and for simplicity ignoring interference between reflections coming from the two mirror boundaries, one should expect reflection from each of them, with a strength of $|(N_1-N_2)/(N_1+N_2)|^2$ where N_1 and N_2 are the complex indices of refraction of the mirror and its surroundings ($N = n+\mathrm{i}\kappa$, where n is the index of refraction and κ is usually referred to as the extinction coefficient. If $n/\kappa \gg 1$, then κ may be neglected in the above calculation). From the latter it is clear that in order to reflect, the mirror material must be immersed in an environment with an index of refraction different than its own, or alternatively, when this is hard to achieve such as for X-ray, the mirror should be constructed to Bragg reflect the light. It is also important to note that even a large transmittance probability does not hinder the experiment as these non interacting photons arrive at detector D1 and thus do not contaminate the small symmetry breaking signal at D2. It is however true that the transmittance probability will have to be verified independently so that the D1 signal may be normalized and consequently so that true values of I_2 and I_1 may be extracted. κ also affects the internal scattering and heating of the mirror. As this process is able to contaminate the small signal at D2 it will be important to suppress it. A small κ ensures that the internal absorption $1-\exp(-2k\kappa x)$ will remain small (where k is the wave vector of the incoming wave and x is simply the propagation distance of the wave within the material). Experimental values for the extinction coefficient in the X-ray region are usually of the order of 10^{-6} to 10^{-7} [23]. Making use of these numbers and a mirror thickness of 100 Å, one finds an absorption of less than 1%. Of course, a more accurate account should also take into consideration factors like the dependence of the extinction coefficient on temperature, errors rising from roughness and contamination of the mirror surface, etc. [23]. For red light, having in general higher extinction coefficients, absorption should be seriously considered.

One should also consider the mechanical properties of such a mirror. Namely, can the mirror be fabricated to have the example frequency of 10 Hz. It is well-known that rectangular or circular plates with clamped edges have a fundamental $(0,0)$ mode frequency of order $C_L h/L^2$ (times 1.654 or 0.4694 for rectangular and circular, respectively), where L is the dimension of an oscillating plate of thickness h and $C_L = \sqrt{E/\rho(1-\nu^2)}$ is the velocity of sound in the plate [24]. E is Young's modulus. Taking for example metals, E is in the order of $10-20\times10^3$ $\mathrm{N/m^2}$, ρ is the density, which for metals is in the order of $10-20\times10^3$ $\mathrm{kg/m^3}$, and ν is Poisson's ratio, which is 0.3 for most materials. Taking the thickness to be 100 Å and the mirror to be of dimension 1 mm, one finds that the frequency will be of the order of 10 Hz as required.

Next, we touch upon the important issue of the vacuum environment of the mirror. Working within the regime of extremely small η in which the foil excitation probability in negligible (*e.g.* from the Debye-Waller factor of $\exp(-\eta^2)$), obviously has its advantages, but also its price: As explained in the caption of Figure 4, the signal $I_2/(I_2+I_1)$ is strongly suppressed for small η values. In such a case, for the experiment to work, different sources of noise (*e.g.* a thermal tail of the foil level population above the ground state) have to be suppressed to the same level. Alternatively, one could work in the foil-excitation regime and gain control over such unwanted excitations, in ways decried previously in this work. However, here also a price must be paid. In such a scenario, it is plain that background gas particles, having more momentum than the photons, would excite the foil in an uncontrollable way into unknown initial states – inhibiting us from isolating localization signals. Consequently, it is evident that the experiment (including mirror preparation) must be conducted in a time much shorter than the mean time separation between background gas collisions with the mirror. This is indeed realizable since low temperature (≈ 1 K) vacuums may reach 10^{-18} mbar [25], which means a particle density of 10^7 $\mathrm{m^{-3}}$ and a hit frequency of 10^3 $\mathrm{s^{-1}}$ for a 1 mm^2 mirror. One would also be able to verify the affect of the background gas by changing the mirror surface area and taking into account the straightforward hit frequency scaling law as a function of the area.

Last, we consider the issue of system preparation. It is clear that for the experimental idea presented in this paper to work, the symmetry change of the mirror during the experiment has to be known. If one is to achieve this through preparing the mirror in the harmonic ground state, one must be able to cool the mirror sufficiently in order to ensure the latter. Indeed, Mancini, Vitali and Tombesi [26], have shown that through radiation pressure modulated by a homodyne feedback which senses the position of an oscillating mirror, one is able to effectively cool the mirror. Their idea has already been realized successfully [27]. In Appendix D it is shown that this method may be extended to temperatures of 1 mK and below. In such a case, one finds that for an η of order one, a 10^9-10^{12} particle mirror can be cooled to its ground state – depending on its Q factor, where $Q=\omega\tau$ and where ω and τ are the frequency and the mechanical relaxation time of the mirror, respectively. It should be noted that even the small reflectance of a 10^9 particle mirror, consisting

for example of a surface of 10 μm $\times$ 10 μm and a 10 atom layer surface, will not hinder the experiment as transmitted photons will not change their symmetry and hence not add to the noise in D2.

Alternatively, the initial state of the mirror can also be a higher state, be it of odd or even symmetry. As explained in Sections 5 and 6, in such a scenario, one would have to resort to energy measurements of the outgoing photon in order to choose only the non excitation events or those in which the symmetry of the foil has not changed. Here also, a larger Q factor would enable such a measurement for larger masses [28]. Taking as a benchmark, an energy detection resolution of 10^{-13} of the photon energy, one finds from Figure 5, that in the region of $\eta = 1$, the experiment can presently be done with a 10^9 (10^5) particle mirror, for X-ray (red) light. One should note that a 10^9 particle object will decohere in very long time scales according to models such as the original GRW proposal [29] – rendering the experiment realistically unsensitive to this low mass range. However, updated models such as the Continuous Spontaneous Localization model [7], predict much shorter collapse times. Moreso, other models such as that of environmental decoherence, predict yet even shorter decoherence times [13], and so it seems that even for the short time scales discussed above in the context of the vacuum, the experiment will be sensitive to many of the models of the second type, already in the mass region of 10^9 particles.

To conclude, analyzing the mirror features, the issue of vacuum and the above two preparation scenarios, and noting that a 10^{10} particle foil oscillator has already been nano-fabricated [30], we find that the suggested experiment stands at the edge of present technology, and some versions of it are already now realizable.

Finally, we discuss environmentally induced decoherence.

8 Observing environmental decoherence

Before the end of this paper, we would like to revisit the issue of the work assumptions. The working assumptions, which have been presented in the beginning of the paper, form the underlying logic behind the hypothesis that the *symmetry experiment* should exhibit sensitivity to all models of the second class. However, the different models of this class have slightly different features and hence require finally a separate examination in order to predict how the *symmetry experiment* would evolve for each model. These model specific analyses will be examined in the future and in the following we present some preliminary considerations. The latter will mainly focus on Decoherence (*i.e.* environmental) as it is perhaps more widely accepted and as it has been suggested that due to its magnitude, it will mask other hypothesized processes (see introduction) and hence will be the main observable of this experiment.

The first parameter to be evaluated if the *symmetry experiment* is to be realized is $\tau_{\rm dec}$ – the time of decoherence. The experimental time resolution must of course be better than $\tau_{\rm dec}$ if we are to observe the transition from Quantum to Classical. From the finite temperature equation $\tau_{\rm dec} = \gamma^{-1}(\lambda_{\rm dB}/\Delta L)^2$ where γ is a relaxation parameter and the other two parameters are the de Broglie wave length and the coherency length [11], it is clear that well isolated macroscopic bound states may be defended against decoherence for long periods of time. Indeed, in the latter reference, Zurek gives the example of a massive Weber bar in cryogenic temperatures. Nevertheless, it is also clear that the specific environment of the experimental realization will have to be scrutinized to great detail in order to arrive at correct estimates for $\tau_{\rm dec}$.

A second issue which will have to be closely examined is the evolution of the initial state into the statistical mixture and the consequential magnitude of the symmetry breaking and its observed signature. In our proposed experiment, the magnitude of the symmetry breaking is simply $2\Delta x$, where Δx is the distance between the center of the "Classical state" and the mean position (in our case at $x = 0$). For example [31,32], if the system-environment Hamiltonian is such that final states (the so-called "pointer states") have exactly the same x-space width as the initial states, the Δx of our experiment and the symmetry breaking signal would disappear. As the "pointer states" become sharper relative to the initial state, the statistical mixture is more pronounced, Δx is larger, and the observed signature in detectors D1 and D2 (as explained in Appendix A) will be larger. Again, as for $\tau_{\rm dec}$, here also there are clear examples of situations in which the relative sharpness of the pointer states is adequate.

9 Outlook

In a sequential paper, we will specifically treat the predictions of the different models of the second type in the context of the *symmetry experiment*. There, we will also address in more detail questions such as that of system preparation and the evolution of the mirror into a statistical mixture of states – time scales and final states.

One should of course also thoroughly examine the mirror model and other realistic mechanisms which are able to produce an asymmetric signal.

As for mirror isolation, schemes superior to the nano-fabricated foil, may include a charged mirror in an ion trap, or a magnetic or diamagnetic mirror in a magnetic trap [38].

Finally, one should note that other, perhaps advantageous, possibilities for the interaction region C, may include large atoms or molecules or perhaps even condensate gases, in a trap with very long coherence times.

10 Summary and conclusion

We have discussed the class of induced localization models, among them *Decoherence*. We have shown that if these models comply with several assumptions, essential to their philosophy, then, a symmetry based experiment should be able to investigate the hypothesized loss of coherency.

$$\frac{|\exp(\mathrm{i}[k(x+2X_{\rm loc})])+\exp(\mathrm{i}[k(x-2X_{\rm loc})])|^2}{|\exp(\mathrm{i}[k(x+2X_{\rm loc})+\pi/2])+\exp(\mathrm{i}[k(x-2X_{\rm loc})+3\pi/2])|^2}=$$

$$\frac{|[\exp(\mathrm{i}2kX_{\rm loc})+\exp(-\mathrm{i}2kX_{\rm loc})]\exp(\mathrm{i}\pi)|^2}{|\exp(\mathrm{i}2kX_{\rm loc})\exp(\mathrm{i}\pi/2)+\exp(-\mathrm{i}2kX_{\rm loc})\exp(\mathrm{i}3\pi/2)|^2}=\frac{\cos^2(2kX_{\rm loc})}{\sin^2(2kX_{\rm loc})}$$

The proposed *symmetry experiment* will hopefully be able to investigate three important regimes: the evolution of an isolated macroscopic quantum system, the transition into localized states, and the different predictions of the various models of the second type.

One of us (R.F.) is grateful for enlightening discussions with Professors Anton Zeilinger, Zeev Vager, Yakir Aharonov, Bill Phillips, Wojciech Zurek, Juan-Pablo Paz and Jeffrey Bub. We are also thankful for helpful comments made by Markus Gangl.

Note added in proofs

We have lately received a number of requests for clarification regarding the fundamental reason behind the fact that the symmetry experiment reveals no "which path" information. It is quite clear that the photon measurement produces no such knowldege as the eigen states of the measurement are parity eigenstates. What seems not to be so clear to some people is why no such traces are left in the foil. In the following we try and clarify this point. What ever the final state of the mirror is, one can express it in the basis of harmonic eigenmodes. In order to conserve symmetry and energy, each such mode is entangled with a specific (symmetry and energy) photon final state (see Eq. (1)). As our measuring device has parity eigen states, it will always collapse the photon into a specific parity state and with it the mirror will collapse into the appropriate harmonic eigenmode, in which there is no which way information as it received no momentum. If the mirror was excited into a higher mode, it has indeed received energy, but energy does not reveal any which path information. Similarly, because of the collapse of the final photon into a parity state, the environment of the mirror (*i.e.* its holders) did not receive any mean momentum. Here, no which path information is ensured by the fact that the momentum uncertainty of the massive holders is much bigger than the $2k$ momentum kick given by the photon.

Appendix A: Localization signal

Let us assume the foil C is localized at distance $|X_{\rm loc}|$ from the $x=0$ symmetry axis.

Let us now assume a normal plane wave $\exp(\mathrm{i}kx)$ where k is the absolute value of the wave number. Dividing away the normalization and other identical factors, and remembering that the phase shifter cancels the phase difference introduced by the beam splitter (here for example we take $\pi/2$), one finds for I_1/I_2 for a single event:

see equation above

where, for simplicity, we have neglected taking account of the expected non-negligible transmittance of the mirror, due to its small thickness.

One should also consider the fact that in a bound state it could be that localizations would cause excitation to higher quantum levels with specific parity, rather than ending up as the localized asymmetric states we are considering here [7]. Hence, in a real experiment, this rate should be calculated and subtracted from the signal.

Appendix B: Debye-Waller factor

Let us calculate the Debye-Waller factor for the foil.

First, we expand the ground state in the momentum basis $|i\rangle=\sum_{k'}|k'\rangle\langle k'|i\rangle$ and note that $\exp(-\mathrm{i}k^{\Delta}x)$ operating on a plane wave state, changes the wave number by an amount k^{Δ} which is simply the difference between the incoming photon wave number k_1 and that of the outgoing photon k_2 *i.e.* $k^{\Delta}=k1+k2$ namely, $\exp(\mathrm{i}k^{\Delta}x)|k'\rangle=|k'-k^{\Delta}\rangle$. Summing over all k' one gets the familiar $|f\rangle=\exp(-\mathrm{i}k^{\Delta}x)|i\rangle$. Now,

$$P_{0\to n}=\Big|\int\Psi_0^{\dagger}(x)(K_++K_-)\Psi_n(x)\Big|^2 \qquad \text{(B.1)}$$

where $K_+=\frac{1}{2}(\exp(-\mathrm{i}k^{\Delta}x)+\exp(\mathrm{i}k^{\Delta}x))$ and $K_-=\frac{1}{2}(\exp(-\mathrm{i}k^{\Delta}x)-\exp(\mathrm{i}k^{\Delta}x))$ are simply the symmetric and anti-symmetric kick operators. The factor $1/2$ in the K operators, which comes from the normalization of the photon wave function, ensures that although different from the standard Mössbauer calculation *i.e.* here we have a kick from both sides, the result stays the same (see Appendix C).

Let us now calculate $P_{0\to 0}$. We note $Q_n(x)=\Psi_n^{\dagger}(x)\Psi_n(x)$ as the density operator and find:

$$\begin{aligned}P_{0\to 0}&=\Big|\int\Psi_0^{\dagger}(x)K_+\Psi_0(x)\Big|^2\\ &\approx\Big|\int Q_0\frac{1}{2}(2-(k^{\Delta})^2x^2)\Big|^2=\Big|\int Q_0-\frac{(k^{\Delta})^2}{2}\int Q_0x^2\Big|^2\\ &=\Big|1-\frac{(k^{\Delta})^2}{2}\langle x^2\rangle_0\Big|^2\approx 1-(k^{\Delta})^2\langle x^2\rangle_0\\ &\approx\exp(-(k^{\Delta})^2\langle x^2\rangle_0)=\exp(-\hbar^2(k^{\Delta})^2/2m\hbar\omega). \qquad \text{(B.2)}\end{aligned}$$

As for this case $k_1=k_2$ since there is no energy transfer, the final result is

$$\exp(-2\hbar^2k_1^2/m\hbar\omega). \qquad \text{(B.3)}$$

The above probability for the foil not to be excited is simply the well known Debye-Waller factor for the case of reflection.

Appendix C: Excitation probabilities

1. In the previous appendix, we presented the classical quantum calculation for the Debye-Waller factor. In the following, we present the same calculation but in the language of annihilation and creation operators, in a way which can be easily expanded to calculate excitation probabilities to all levels. Furthermore, in this appendix we rigorously describe how the system Hamiltonian allows for excitations to both symmetric and anti-symmetric states.

Let us consider H the total coherent scattering Hamiltonian of our system $H_{\rm light} + H_{\rm c.m.-mirror} + H_{\rm polarization} + H_{\rm interaction}$ to be:

$$\hbar\nu(\hat{a}_+^\dagger\hat{a}_+ + \hat{a}_-^\dagger\hat{a}_- + 1) + \hbar\omega\left(\hat{b}^\dagger\hat{b} + \frac{1}{2}\right) + \hbar\mu(\hat{c}^\dagger\hat{c} + \frac{1}{2}) - \alpha E^2 \quad \text{(C.1)}$$

where ν, ω and μ are the frequencies of the light, mirror and polarization, respectively, and $\hat{a}$, $\hat{b}$ and $\hat{c}$, are the usual creation and annihilation operators. $\hat{a}_+$ and $\hat{a}_-$ denote photons going right and left along the x-axis of the experimental set-up described earlier. α is the polarizability and E is the electric field of the incoming light, which is simply:

$$\mathbf{E} = \epsilon\{\hat{a}_+ e^{(ikx)} + \hat{a}_- e^{(-ikx)} - \hat{a}_+ e^{(-ikx)} - \hat{a}_- e^{(ikx)}\}\tilde{e} \quad \text{(C.2)}$$

where $\tilde{e} = i\sqrt{\hbar\nu/2\epsilon_0 V}$ and ϵ is the polarization vector ($\mathbf{P} = \alpha\mathbf{E}$ is usually denoted as the polarization of the medium. Here, for simplicity, we neglect the variation of $\mathbf{P}$ as a function of x. For wavelengths short compared to the thickness of the mirror, this will of course have to be taken into account. We also note that expressing $\mathbf{P}$ in terms of $(\hat{c}+\hat{c}^\dagger)$ as is usually done, and using the adiabatic approximation $d\hat{c}/dt = i[H,\hat{c}] = 0$ to calculate $\hat{c}$, gives the same result). Hence we find for $H_{\rm int}$,

$$-\alpha\{(2\hat{a}_+\hat{a}_- - \hat{a}_+\hat{a}_+^\dagger - \hat{a}_-\hat{a}_-^\dagger - \hat{a}_+^\dagger\hat{a}_+ + 2\hat{a}_+^\dagger\hat{a}_-^\dagger - \hat{a}_-^\dagger\hat{a}_-) + (\hat{a}_+ - \hat{a}_-^\dagger)^2 e^{(i2kx)} + (\hat{a}_- - \hat{a}_+^\dagger)^2 e^{(-i2kx)}\}\tilde{e}^2. \quad \text{(C.3)}$$

Noting that the first term is responsible for off-energy-shell (virtual) photons and phase shifts, we write:

$$V_{\rm eff} = \alpha\tilde{e}^2\{(\hat{a}_+\hat{a}_-^\dagger + \hat{a}_+^\dagger\hat{a}_-)2\cos(2kx) + i(\hat{a}_+\hat{a}_-^\dagger - \hat{a}_+^\dagger\hat{a}_-)2\sin(2kx)\}. \quad \text{(C.4)}$$

We see here, how $V_{\rm eff}$ has the ability to excite the foil into a symmetric state while leaving the photon wave function symmetric, or alternatively, to excite the foil into an anti-symmetric state while changing the photon state from symmetric to anti-symmetric. Expressing the latter formally, we note:

$$|\Psi(0)\rangle = \frac{1}{\sqrt{2}}|0\rangle_m(|1\rangle|0\rangle + |0\rangle|1\rangle)_p \quad \text{(C.5)}$$

where m means "mirror" and p "photon". As $(i/\hbar)(d/dt|\Psi(t)\rangle = H_0|\Psi(t)\rangle + V_{\rm eff}|\Psi(t)\rangle$, the changes in the wave function will be proportional to:

$$2\cos(k^\Delta x)|0\rangle_m\frac{1}{\sqrt{2}}(|1\rangle|0\rangle + |0\rangle|1\rangle)_p + 2i\sin(k^\Delta x)|0\rangle_m\frac{1}{\sqrt{2}}(|1\rangle|0\rangle - |0\rangle|1\rangle)_p \quad \text{(C.6)}$$

where k^Δ has been defined in the previous appendix. The relative excitation probabilities will thus be:

$$P_{0\to n(\rm even)} = \frac{\alpha^2\tilde{e}^4}{\hbar^2}|\langle n|\cos(k^\Delta x)|0\rangle|^2 \quad \text{(C.7)}$$

and

$$P_{0\to n(\rm odd)} = \frac{\alpha^2\tilde{e}^4}{\hbar^2}|\langle n|\sin(k^\Delta x)|0\rangle|^2 \quad \text{(C.8)}$$

Let us calculate P.

In the Lamb-Dicke limit [33], $\eta = \sqrt{E_{\rm r}/\hbar\omega} = k^\Delta\sqrt{\hbar/2m\omega} = 4\pi W/\sqrt{2}\lambda \ll 1$, where η is the Lamb-Dicke parameter, W the size of the harmonic potential ground state, λ the wavelength of the impinging light, m and ω the mass and frequency of the oscillator, and $E_{\rm r}$ the recoil energy. As can be readily seen, in this limit the ground state size (or recoil energy) is much smaller than the wavelength of the incoming beam (or oscillator energy spacing). Hence, an expansion of the excitation matrix element in powers of η, is allowed. Making use of our typical numbers (*i.e.* $m = 10^{15}$ particles and $\omega = 2\pi\times 10$ Hz), one finds that our system is within this limit for the full range of X-ray to red light. This limit is of course very different from our initial demand of $\sqrt{\hbar/m\omega} \gg \lambda$, which results for the same mass and frequency range, in extremely low values for the harmonic oscillator frequency. It is also very different than the parameter regime which one would need in order to observe the described form of R. We now turn to calculate the probability for excitation to the even and odd states. Using the results of the previous appendix and the above definition of η, and using the normal convention for the position operator $\hat{x} = (\hbar/2m\omega)^{\frac{1}{2}}(\hat{a} + \hat{a}^\dagger)$, we find:

$$P_{0\to n(\rm even)} = \sum_n|\langle n|\cos[\eta(\hat{a}+\hat{a}^\dagger)]|0\rangle|^2 \approx \sum_n|\langle n|1 - \frac{1}{2}\eta^2(\hat{a}+\hat{a}^\dagger)^2|0\rangle|^2 = 1-\eta^2, \quad \text{(C.9)}$$

$$P_{0\to n(\rm odd)} = \sum_n|\langle n|\sin[\eta(\hat{a}+\hat{a}^\dagger)]|0\rangle|^2 \approx \sum_n|\langle n|\eta(\hat{a}+\hat{a}^\dagger)|0\langle|^2 = \eta^2, \quad \text{(C.10)}$$

where we expanded up to second order in η, and where all probabilities should be multiplied by $\alpha^2\tilde{e}^4/\hbar^2$ and by the total photon scattering probability Ω. A very small Ω (*e.g.* due to small thickness), will cause the overall intensity in D2 to be much smaller than that calculated above, as P are calculated only for the portion of the photons which are scattered.

2. In order to calculate $R_{\rm bound}$, one simply needs to calculate $I_2/(I_2+I_1)$, as we have already calculated $P_{0\to 0}$ in the previous appendix.

As noted, $I_2/(I_2+I_1)$ is the probability that a click is received in detector D2 when a localizing event has occurred at the mirror. From Appendix A, we have that a specific localization at $X_{\rm loc}$ gives rise to $I_2/(I_2+I_1) = \sin^2(4\pi X_{\rm loc}/\lambda)$. In order to average over all possible values and probabilities of $X_{\rm loc}$, one has to integrate over the localization location probability distribution $f(X_{\rm loc})$ which is nothing more than the initial state position distribution

$$f(X_{\rm loc}) = \Psi_0^\dagger(X_{\rm loc})\Psi_0(X_{\rm loc}) \tag{C.11}$$

where in our example Ψ_0 is simply the harmonic ground state $(m\omega/\pi\hbar)^{1/4}\exp(-m\omega x^2/2\hbar)$.

Defining, $a=\sqrt{m\omega/\hbar}$ and $b=8\pi/\lambda$ we find that the integral that needs to be evaluated is:

$$\frac{I_2}{I_2+I_1} = \frac{a}{\sqrt{\pi}}\int_{-\infty}^{+\infty}\exp(-a^2{X_{\rm loc}}^2)\sin^2\left(\frac{b}{2}X_{\rm loc}\right)\mathrm{d}X_{\rm loc}.$$

As

$$\int_0^\infty \exp(-a^2x^2)\cos(bx) = \int_0^\infty \exp(-a^2x^2)\left(1-2\sin^2\left(\frac{b}{2}x\right)\right)$$

and as

$$\int_0^\infty \exp(-a^2x^2) = \frac{\sqrt{\pi}}{2a}$$

and

$$\int_0^\infty \exp(-a^2x^2)\cos(bx) = \frac{\sqrt{\pi}\exp(-b^2/4a^2)}{2a}$$

one finds:

$$\int_{-\infty}^{+\infty}\exp(-a^2x^2)\sin^2(\frac{b}{2}x) = \frac{\sqrt{\pi}}{2a}(1-\exp(-b^2/4a^2)).$$

Hence we find: $I_2/(I_2+I_1) = (1-\exp(-16\pi^2/\lambda^2a^2)/2$ and

$$R_{\rm bound} = \frac{1-P_{0\to 0}}{I_2/(I_2+I_1)} = 2\frac{1-\exp(-8\pi^2/\lambda^2a^2)}{1-\exp(-16\pi^2/\lambda^2a^2)}\,. \tag{C.12}$$

Appendix D: Ground state cooling

In one of the experimental schemes proposed in this paper, the center of mass of the mirror has to be prepared in its motional quantum ground state. Cooling a macroscopic object to its motional gound state seems to be a prohibitive task, since up to now it has been achieved only for single ions in rf-traps [34] and atoms in optical lattices [35]. Moreover, it is impractical to adopt here usual cryogenic techniques, because it would make very difficult to use the mirror within the interferometer. Nonetheless, it has been recently theoretically proposed [26], and already experimentally verified [27], that it is possible to cool an oscillating mirror of an optical Fabry-Perot cavity using the radiation pressure. This idea has been proposed as a new technique to cool room-temperature massive objects, alternative to standard cryogenics, and in the experiment of reference [27], the mirror temperature has been lowered by a factor 40. Here we show that, in the case of a mirror with a very high-Q mechanical factor, the same method could be applied in principle, to cool the harmonically oscillating mirror even to its quantum ground state. When the mechanical frequency ω is much smaller than the resonance frequency of the electromagnetic mode in the cavity $\omega_{\rm c}$, retardation effects, the Doppler frequency shift and the Casimir effect are negligible and the system is described by the Hamiltonian

$$H = \hbar\omega\hat{b}^\dagger\hat{b} + \hbar\omega_c\hat{a}^\dagger\hat{a} - \hbar G\hat{a}^\dagger\hat{a}\left(\hat{b}+\hat{b}^\dagger\right), \tag{D.1}$$

where $\hat{a}$ and $\hat{b}$ are the annihilation operators of the cavity mode and of the mirror respectively, and $G = \sqrt{\hbar\omega_{\rm c}^2/2m\omega L^2}$ (L is the length of the Fabry-Perot cavity) [26]. When the cavity mode is externally driven by a sufficiently intense laser field, the system reaches a quasi-classical steady state with the cavity mode in a coherent state $|\beta_{\rm s}\rangle$ ($\beta_{\rm s}\gg 1$) and with a displaced equilibrium position for the mirror. The quantum fluctuations around this steady state are then well-described by a linearized Hamiltonian, which, in the interaction picture with respect to the unperturbed cavity mode Hamiltonian, reads [26]

$$H = \hbar\omega\hat{b}^\dagger\hat{b} - 2\hbar G|\beta_{\rm s}|Y_\varphi\left(\hat{b}+\hat{b}^\dagger\right), \tag{D.2}$$

where $Y_\varphi = (\hat{a}\mathrm{e}^{\mathrm{i}\varphi} + \hat{a}^\dagger\mathrm{e}^{-\mathrm{i}\varphi})/2$ is the cavity field mode quadrature with phase $\varphi = \arg(\beta_{\rm s})$. This Hamiltonian shows that the dynamics of a generic field quadrature $Y_\delta \neq Y_\varphi$ is sensitive to the position of the mirror $x = \sqrt{\hbar/2m\omega}(\hat{b}+\hat{b}^\dagger)$ and therefore a continuous homodyne measurement of Y_δ provides an effective continuous monitoring of the mirror position. The basic idea of the cooling scheme is to use this continuous position measurement by applying a feedback loop able to decrease the position fluctuations. Due to the continuous nature of the measurement and to the effect of the harmonic potential coupling the mirror position with its momentum, feedback will realize an effective phase-space localisation. With this respect, the scheme is a sort of "continuous version" of the

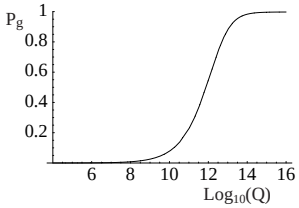

Fig. 6. Probability to prepare the harmonic ground state of the mirror $P_{\rm g}$ as the stationary state of the feedback process, versus the mechanical quality factor $Q = \omega/\gamma$. The curve refers to an initial temperature $T = 300$ K, to an homodyne measurement efficiency $\eta_{\rm h} = 0.99$ and to a mirror oscillation frequency $\omega = 1$ kHz.

stochastic cooling methods employed in particle accelerators and recently studied also for trapped atoms [36,37]. The best way to feed back the homodyne photocurrent is to use it as a driving term for the momentum [26], and the easiest way to realize it, is to use just the scheme experimentally employed in reference [27]. In this case an effective momentum driving is obtained by using the radiation pressure on the back side of the mirror, exerted by an external laser whose intensity is modulated by the *derivative* of the homodyne photocurrent.

The dynamics of the mirror in the presence of the continuous homodyne-mediated feedback can be derived, and, in the limit of negligible feedback delay time, it is described by a Markovian master equation [26,37]. The relevant point is that when the mechanical frequency ω is much larger than the mechanical damping γ and than the feedback gain g (see [26]), the approach to the stationary state in the presence of feedback can be described by averaging over the harmonic oscillations which means choosing the rotating frame at frequency ω. In this rotating frame, the mirror master equation of reference [26] reduces to

$$\dot{\rho} = \frac{(\gamma+g)}{2}(N+1)\left(2\hat{b}\rho\hat{b}^{\dagger} - \hat{b}^{\dagger}\hat{b}\rho - \rho\hat{b}^{\dagger}\hat{b}\right) + \frac{(\gamma+g)}{2}N\left(2\hat{b}^{\dagger}\rho\hat{b} - \hat{b}\hat{b}^{\dagger}\rho - \rho\hat{b}\hat{b}^{\dagger}\right), \quad \text{(D.3)}$$

where

$$N = \frac{1}{\gamma+g}\left[\frac{\gamma}{\exp\{\hbar\omega/kT\}-1} + \frac{4G^2|\beta_{\rm s}|^2}{\gamma_{\rm b}} + \frac{g^2\gamma_b}{64\eta_{\rm h}G^2|\beta_{\rm s}|^2} - \frac{g}{2}\right]$$

($\gamma_{\rm b}$ is the cavity decay rate and $\eta_{\rm h}$ is the efficiency of the homodyne measurement). This expression for N corresponds to that of reference [26] except that we have considered the optimal case when the measured field quadrature is the one orthogonal to Y_φ ($\phi = -\pi/2$ in [26]) and we have used the exact expression of the mean thermal vibrational number instead of the high-temperature limit $kT/\hbar\omega - 1/2$.

The stationary state of the master equation (D.3) is just a thermal state with effective mean vibrational number N. The interesting point is that, if the oscillating mirror has a very good mechanical quality factor $Q = \omega/\gamma$, the feedback gain g can be chosen so that the mean vibrational number N can become arbitrarily close to zero, that is, the motional ground state can be prepared with a probability close to one. This fact is illustrated by Figure 6, where the ground state probability $P_{\rm g} = (1+N)^{-1}$ is plotted *versus* the mechanical quality factor Q. The curve refers to a homodyne-mediated feedback loop with efficiency $\eta_{\rm h} = 0.99$ and optimal gain $g \simeq 20$ Hz, which is applied to a mirror initially at room temperature. Unfortunately, one has an acceptable preparation of the ground state of the mirror only for extremely large values of Q ($P_{\rm g} \simeq 0.95$ for $Q = 10^{13}$). However the curve of Figure 6 does not change appreciably for mirror frequencies in the range 1 kHz $\leq \omega \leq$ 100 MHz, and this is interesting, because it implies the possibility to perform the experiment with a high-Q mirror composed of 10^{12} particles, which is a feasible nanofabrication project [30]. In fact, as we have seen above, one has to consider a Lamb-Dicke parameter $\eta \simeq 1$ in order not to have a signal suppression. Using X-ray photons, and assuming a mirror oscillation frequency $\omega = 1$ kHz, this implies a mirror mass $m \simeq 10^{-15}$ kg, *i.e.* a 10^{12} particles mirror.

The above feedback scheme could be implemented just using the same experimental scheme of reference [27], based on an optical Fabry-Perot cavity, which for example can be collinear with the interferometer. In this case one needs a mirror foil with a good reflectivity for optical wavelengths; the other "fixed" mirror of the cavity needs to have a good reflectivity at optical wavelengths too, while it has to be essentially transparent in the X-ray region, so that it does not affect the interferometric detection of the decoherence-induced symmetry breaking. Alternatively, one may use a non-collinear cavity (two additional mirrors instead of one), or preferably, simply make use of interferometer itself to be part of the feedback system before it is part of the measurement. Indeed, it is designed to detect minute mirror changes in order to be sensitive to the hypothesized localizations.

Finally, it is important to note another feature of the high-Q mirror. The heating time starting from the ground state is essentially given by $t_{\rm heat} = \hbar\omega/\gamma kT = \hbar Q/kT$; using the required value $Q = 10^{13}$, one has $t_{\rm heat} \simeq 30$ s, which means that with a high-Q mechanical mirror, heating does not represent an experimental problem.

References

1. R. Feynman, R. Leighton, M. Sands, *The Feynman Lectures on Physics* (Addison Wesley, 1965), Vol III.
2. L. de Broglie, *La Thermodynamique de la Particule Isolée*, (Gauthier-Villars Paris, 1964), p. v; M. Mugur-Schachter (de Broglie's student), private communication; see also: O. Costa de Beauregard, *Waves and Particles in Light and Matter*, edited by van der Merwe Alwyn, Garrucio Augusto (Plenum Press, 1990).
3. D. Bohm, Phys. Rev. **85**, 166 (1952); 180 (1952); D. Bohm, B.J. Hiley, *The Undivided Universe* (Routledge Press, 1993); see also: David Z. Albert, Scientific American (May, 1994); it should be noted that since non-locality is probably here to stay, the notion of reality, which was

achieved by Bohm, does not fully retrieve our classical notion of reality. This point was put forward by: B.J. Englert, M.O. Scully, G. Sussmann, H. Walther, Z. Naturforsch **47a**, 1175 (1992).
4. B. Millard, A. Shimony, in *Bohmian mechanics and Quantum Theory: An Appraisal*, edited by Cushing *et al.* (Kluwer Academic Publishers, 1996), p. 251 and references therein.
5. A. Peres, *Quantum Theory: Concepts and Methods* (Kluwer Academic Publishers, 1993); *Sixty-Two Years of Uncertainty*, edited by A.I. Miller (Plenum Press, 1990); J.S. Bell, *Speakable and Unspeakable in Quantum Mechanics* (Cambridge University Press, 1987); F. Selleri, *Wave-Particle Duality & QM versus Local Realism* (Plenum Press, 1992 & 1988); J. Bub, *Interpreting the Quantum World* (Cambridge University Press, 1997).
6. E.P. Wigner, Am. J. Phys. **31**, 6 (1963).
7. P. Pearle, E. Squires, Phys. Rev. Lett. **73**, 1 (1994) and references therein.
8. R. Folman, Z. Vager, Found. Phys. Lett. **8**, 345 (1995).
9. D. Bohm, B.J. Hiley, *The Undivided Universe* (Routledge Press, 1993), p. 346.
10. R. Penrose, Gen. Relat. Gravit. **28**, 581 (1996); see also references in [7,16].
11. W.H. Zurek, Phys. Today (1991) p. 36, and references therein. This school of thought originated with H.D. Zeh, Found. Phys. **1**, 69 (1970); see also references in [16].
12. This is a direct result of the fact that the interaction Hamiltonian is considered to be dependent on x. Hence, a superposition in x (well-localized in p) is expected to environmentally decohere much faster then a superposition in p (well-localized in x).
13. This is a point still debateful. See for example: D. Giulini *et al.*, *Decoherence and the Appearance of a Classical World in Quantum Theory* (Springer, 1996); where in pages 57-58 calculations done by Joos, Zeh (1985) and Tegmark (1993) are presented. These calculations show that GRW and Gravitational collapse will be masked by the interaction with the environment unless one achieves extreme conditions of isolation. However, due to the experimental difficulties, it is unclear to us that the predicted magnitude and time scale of environmental decoherence has been sufficiently confirmed.
14. See for example a recent Electron double slit experiment with a controllable Welcher Weg detector: R. Schuster *et al.*, Nature **385**, 417 (1997).
15. D. Bouwmeester *et al.*, in *Gravitation and Relativity at the turn of the Millennium*, edited by N. Dadhich, J. Narlikar (IUCAA press, India, 1998), p. 333.
16. Z. Vager, Chem. Phys. Lett. **273**, 407 (1997) and references therein.
17. M. Brune *et al.*, Phys. Rev. Lett. **77**, 4887 (1996).
18. S. Bose *et al.*, Phys. Rev. A **59**, 3204 (1999) and references therein.
19. S. Bose *et al.*, Phys. Rev. A **56**, 4175 (1997) and references therein.
20. I. Tittonen *et al.*, Phys. Rev. A **59**, 1038 (1999).
21. See for example: "Conscious observers have lost their monopoly... The environment can also monitor a system... such monitoring causes decoherence, which allows the familiar approximation known as classical objective reality..." in reference [11].
22. M.O. Scully *et al.*, Nature **351**, 111 (1991) and references therein.
23. See for example, E.D. Palik, *Handbook of Optical Constants of Solids* (Academic Press, 1985), Vols. I & II and references therein.
24. See for example, T.D. Rossing, N.H. Fletcher, *Principles of Vibration and Sound* (Springer-Verlag, 1994) and references therein.
25. See for example, G. Gabrielse *et al.*, Phys. Rev. Lett. **65**, 1317 (1990).
26. S. Mancini, D. Vitali, P. Tombesi, Phys. Rev. Lett. **80**, 688 (1998).
27. P.F. Cohadon *et al.*, Phys. Rev. Lett. **83**, 3174 (1999).
28. V.B. Braginsky, F.Ya. Khalili, K.S. Thorne, *Quantum mesurements* (Cambridge University Press, Cambridge, 1992), p. 15.
29. See for example in *Speakable and Unspeakable in Quantum Mechanics* (J.S. Bell, Cambridge Press, 1987), p. 202 and references therein.
30. A.N. Cleland, M.L. Roukes, Appl. Phys. Lett. **69**, 2653 (1996).
31. W.G. Unruh, W.H. Zurek, Phys. Rev. D **40**, 1071 (1989).
32. W.H. Zurek, S. Habib, J.P. Paz, Phys. Rev. Lett. **70**, 1187 (1993).
33. See for example: J.I. Cirac *et al.*, Phys. Rev. A **46**, 2668 (1992) and references therein.
34. F. Diedrich *et al.*, Phys. Rev. Lett. **62**, 403 (1989); C. Monroe *et al.*, Phys. Rev. Lett. **75**, 4011 (1995); E. Peik *et al.*, Phys. Rev. A **60**, 439 (1999); Ch. Roos *et al.*, Phys. Rev. Lett. **83**, 4713 (1999).
35. S.E. Hamann *et al.*, Phys. Rev. Lett. **80**, 4149 (1998).
36. M.G. Raizen *et al.*, Phys. Rev. A **58**, 4757 (1998).
37. S. Mancini, D. Vitali, P. Tombesi, Phys. Rev. A **61**, 053404 (2000).
38. A.K. Geim *et al.*, Nature **400**, 323 (1999).